Low-mass star formation in Lynds 1333

M. Kun,[1★] S. Nikolić,[2] L. E. B. Johansson,[3] Z. Balog[4]† and A. Gáspár[5]

[1]Konkoly Observatory, H-1525 Budapest, PO Box 67, Hungary
[2]Departamento de Astronomía Universidad de Chile, Casilla 36-D, Santiago, Chile
[3]Onsala Space Observatory, S-439 92 Onsala, Sweden
[4]Steward Observatory, University of Arizona, 933 N. Cherry Av., Tucson, AZ 85721, USA
[5]University of Szeged, Dómtér 9, Szeged H-6720, Hungary

ABSTRACT

Medium-resolution optical spectroscopy of the candidate young stellar objects associated with the small, nearby molecular cloud Lynds 1333 revealed four previously unknown classical T Tauri stars, two of which are components of a visual double, and a Class I source, IRAS 02086+7600. The spectroscopic data, together with new V, R_C, I_C photometric and 2MASS J, H, and K_s data allowed us to estimate the masses and ages of the new T Tauri stars. We touch on the possible scenario of star formation in the region. L 1333 is one of the smallest and nearest known star-forming clouds, therefore it may be a suitable target for studying in detail the small-scale structure of a star-forming environment.

Key words: stars: formation – stars: pre-main-sequence – ISM: clouds – ISM: individual: L 1333.

1 INTRODUCTION

Filamentary molecular clouds with embedded dense cores form a remarkable subset of star-forming clouds in our Galactic environment (e.g. Onishi et al. 1996; Hily-Blant et al. 2005; Nielbock & Chini 2005). Young stellar objects (YSOs) are associated with several cores along the filaments. The formation scenario of the filaments and stars within them, however, are not well understood. The filaments may be parts of shells, swept up by powerful stellar winds or supernovae (e.g. Kiss, Moór & Tóth 2004), or may result from fragmentation of sheet-like structures (Hartmann 2002), or may be shaped by large-scale flows like the Galactic rotation (Koda et al. 2006). Detailed studies of their density and velocity structures, as well as the properties of the YSOs born in them may help understand their formation and evolution.

Lynds 1333, a small dark cloud of opacity class 6 (Lynds 1962) in Cassiopeia, at $(l, b) = (128\overset{\circ}{.}88, +13\overset{\circ}{.}71)$ is part of a filamentary complex. According to the available observations L 1333 is starless, and thus has been included in several studies of starless cores (e.g. Lee, Myers & Tafalla 1999, 2001; Lee, Myers & Plume 2004). Obayashi et al. (1998, hereinafter referred to as Paper I), studied first this cloud. They derived a distance of 180 ± 20 pc from the Sun using Wolf diagram method. Their ^{13}CO and C^{18}O observations have shown L 1333 to be part of a long, filamentary molecular structure, stretching from $l \sim 126^\circ$ to 133° and from $b \sim +13^\circ$ to $+15^\circ$, and referred to this molecular complex as *L 1333 molecular cloud*. The angular extent of the molecular complex corresponds to a length of some 30 pc at a distance of 180 pc. Kiss et al. (2004) found that the L 1333 complex is part of a giant far-infrared loop GIRL G 126+10.

Recent star formation in the L 1333 molecular cloud complex has been indicated by the presence of the *IRAS* source IRAS 02086+7600, whose *IRAS* colour indices are indicative of a Class I protostar, nevertheless it coincides with a faint star in the *Digitized Sky Survey* image. Due to its appearance as an optically visible star with large far-infrared excess several authors considered this object as a possible evolved star. Fujii, Nakada & Parthasarathy (2002) included IRAS 02086+7600 in a multiband photometric survey for candidate post-AGB stars. They could not confirm the post-AGB nature of the star, and noted that it may be an ultracompact H II region, or a post-AGB star, or a YSO. IRAS 02086+7600 appeared as a possible planetary nebula in the target lists of Preite-Martinez (1988) and Van de Steene & Pottasch (1995).

Based on its *IRAS* colours, Slysh et al. (1994) included this object, as a candidate ultracompact H II region, in their search for OH maser emission. They detected it as a thermal OH source at the velocity of 3.1 km s^{-1}. The molecular maps presented in Paper I revealed that this *IRAS* source is projected on a dense C^{18}O core of a nearby molecular cloud whose radial velocity is +3.0 km s^{-1}, same as that of the OH source, suggesting that IRAS 02086+7600 most probably is a low-mass YSO. The C^{18}O spectrum observed at its position exhibited a wing-like feature, indicative of molecular outflow (Paper I). No known Herbig–Haro object is associated with this source.

★E-mail: kun@konkoly.hu
†On leave from University of Szeged, Department of Optics and Quantum Electronics, Dómtér 9, Szeged H-6720, Hungary.

In addition to IRAS 02086+7600, 18 Hα emission stars have been detected in objective prism Schmidt plates in the region of L 1333 (Paper I). Three of these stars are associated with the *IRAS* point sources IRAS F02084+7605, 02103+7621 and 02368+7453.

The aim of this study is to establish an elementary data base on the star-forming activity of the L 1333 complex. We observed the optical spectra of the candidate YSOs in order to establish their pre-main-sequence nature and their spectral types. We also performed optical photometry of the objects in order to determine their luminosities and positions in the Hertzsprung–Russell diagram (HRD). We describe our observational data in Section 2. Our results on the properties of the observed stars, a short description of the large-scale environment of the cloud and the possible star formation scenario are presented in Section 3. Section 4 gives a short summary.

2 OBSERVATIONS AND RESULTS

2.1 Spectroscopy

All the PMS star candidate Hα emission objects and *IRAS* sources listed in Paper I were observed on 2001 January 4, using the ALFOSC spectrograph installed on the 2.5-m Nordic Optical Telescope in the Observatorio del Roque de los Muchachos in La Palma. The spectra were taken through grism 8, giving a dispersion of 1.5 Å pixel^{-1} over the wavelength region 5800–8350 Å. Using a 1-arcsec slit, the spectral resolution was $\lambda/\Delta\ \lambda \approx 1000$ at $\lambda =$ 6560 Å. The exposure times of 900 s for the Hα emission stars resulted in signal-to-noise ratio (S/N) $\gtrsim$ 100. For the much fainter IRAS 02086+7600 the exposure time was 2400 s, resulting in S/N $\approx$ 20. Spectra of helium and neon lamps were observed before and after each stellar observation for wavelength calibration. We observed a series of spectroscopic standards for spectral classification purposes. IRAS 02086+7600 was also observed on 2005 September 13, using the CAFOS instrument on the 2.2-m telescope of Calar Alto Observatory. Using the grism R-100, the observed part of the spectrum covered the wavelength interval 5800–9000 Å. The spectral resolution of CAFOS observation, using a 1.5-arcsec slit, was $\lambda/\Delta\lambda \approx 1000$ at $\lambda = 8500$ Å. The exposure time 2400 s resulted in S/N $\approx$ 7 at 8500 Å. We reduced and analysed the spectra using standard IRAF routines.

We confirmed the pre-main-sequence nature of three candidates listed in Paper I: OKS Hα 5, 6 and 16, all coinciding with *IRAS* point sources and projected on the molecular clouds. The other candidate Hα objects listed in Paper I proved to be field stars without prominent Hα emission and Li I absorption. We found by chance during the observations that a faint star some 1.8-arcsec south-southeast of OKS Hα 6, associated with IRAS 02103+7621, was also a pre-main-sequence star. We refer to the two components as OKS Hα 6 N and OKS Hα 6 S, respectively.

The wavelength range of ALFOSC spectra was suitable for determining several flux ratios defined as tools for spectral classification by Kirkpatrick, Henry & McCarthy (1991), Martín & Kun (1996) and Preibisch, Guenther & Zinnecker (2001). We measured these spectral features on the spectra of our stars, and calibrated them against the spectral type and luminosity class by measuring them in a series of standard stars observed during the same run. The accuracy of the two-dimensional spectral classification, estimated from the range of spectral types obtained from different flux ratios, is ±1 subclass (for further details of spectral classification, see Kun et al. 2004).

Results of the spectroscopy are presented in Table 1. In addition to the derived spectral types we present the equivalent widths (EWs) of the Hα and Li I lines in Å, the 10 per cent-width of the Hα line in km s^{-1}, as well as list the additional emission lines observed in the spectra. The uncertainties given in parentheses have been derived from the repeatability of the measurements. The real uncertainties of the Li I EWs may be higher due to the blending of the line with neighbouring absorption or emission features (Ca I λ 6718, [S II] λ 6717). The spectra, normalized to the continua, are shown in Fig. 1.

Both Fig. 1 and Table 1 show that OKS Hα 5, OKS Hα 6 N, OKS Hα 6 S and OKS Hα 16 are classical T Tauri stars (CTTS). Their spectral types are K or M, and their Hα emission lines fulfil the criteria established for the CTTSs by Martín (1997) [i.e. W(Hα) exceeds the threshold value of 5 Å for K-type stars and 10 Å for M-type stars] and by White & Basri (2003) (the width of the Hα emission line 10 per cent above the continuum level is significantly larger than 300 km s^{-1}). The spectral types were converted into effective temperatures T_{eff} following Kenyon & Hartmann (1995) for luminosity class V, and de Jager & Nieuwenhuijzen (1987) for luminosity classes IV and III. The adopted T_{eff} values are listed in Table 3.

IRAS 02086+7600 displays an emission spectrum, containing strong Hα and several forbidden lines, as well as the Ca II triplet in the CAFOS spectrum. The spectral resolution and the S/N of the spectra are insufficient for identifying absorption features, suitable for spectral classification. In particular, no TiO band, conspicuous in M-type spectra, can be seen, suggesting that its spectral type is probably earlier than M0. The large number of forbidden lines resembles Class I objects (Kenyon et al. 1998; White & Hillenbrand 2004), thought to be either younger than, or identical with the youngest CTTSs. The high far-infrared excess of Class I objects suggests that the central star and its accretion disc are embedded in a dusty

Table 1. Results of spectroscopy.

Star	IRAS name	Spectral type	EW (Hα) (Å)	W(10 per cent) (Hα) (km s^{-1})	EW (Li I) (Å)	Other emission lines
–	02086+7600[a]	<M0	−44.8 (0.5)	570 (10)	–	[O I] 6300, 6363; [S II] 6717, 6731; [N II] 6548, 6584; [Fe II] 7155; [Ca II] 7323; [Ni II] 7378
–	02086+7600[b]		−34.0 (1.0)	760 (20)	–	[O I] 6300, 6363; [S II] 6717, 6731; [Fe II] 7155; [Fe II] 7319; O I 8446; Ca II 8498, 8542, 8662
OKS Hα 5	F02084+7605	M0.5IV	−25.1 (0.5)	610 (12)	0.47 (0.02)	
OKS Hα 6 N	02103+7621	K7V	−51.5 (0.5)	710 (10)	0.40 (0.02)	
OKS Hα 6 S	02103+7621	M2IV	−42.3 (1.0)	465 (15)	0.13 (0.02)	[O I] 6300, 6363; He I 5873, 6678; [S II] 6717, 6731
OKS Hα 16	02368+7453	K7III	−8.0 (0.2)	520 (15)	0.71 (0.02)	

[a]ALFOSC spectrum, 2001; [b]CAFOS spectrum, 2005.

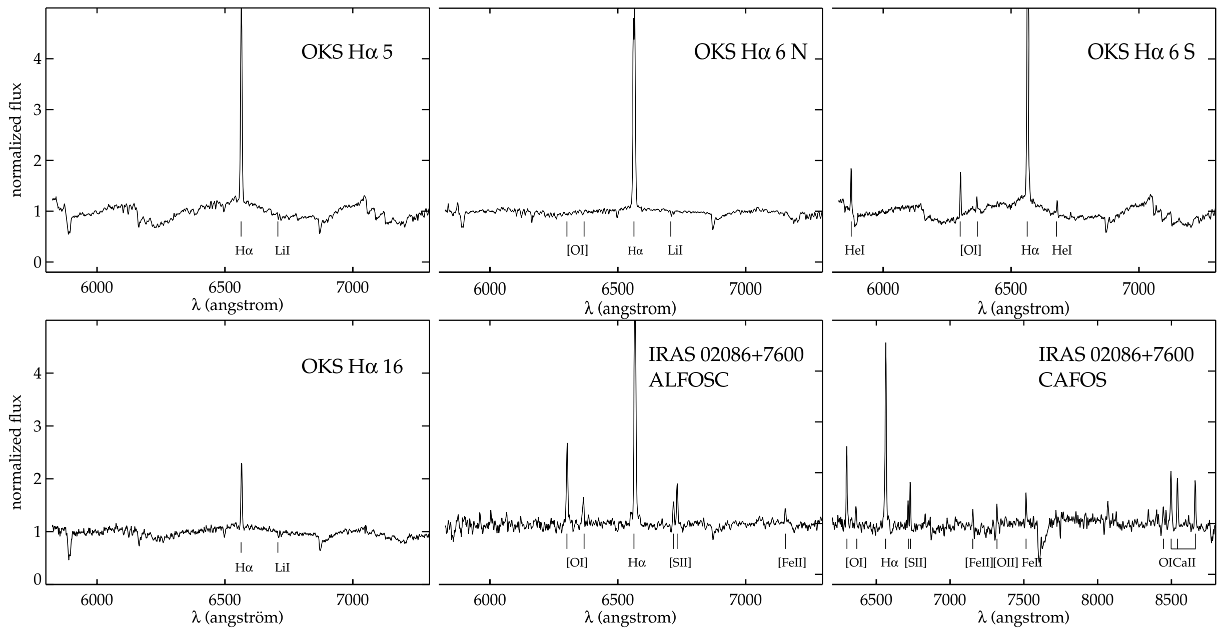

Figure 1. Optical spectra of the YSOs associated with the L 1333 molecular complex.

envelope. Optical photons from such a source escape through the polar cavities of the envelope, cleared by the protostellar wind. Several Class I sources cannot be detected at optical wavelengths, and several others are extended, suggesting that starlight, scattered from the circumstellar dust, contributes to their optical flux (e.g. Eisner et al. 2005). The star-like appearance of IRAS 02086+7600 suggests that one of its polar cavities lies close to our line of sight. The extremely broad Hα emission line supports this assumption.

2.2 V, $R_{\rm C}$, $I_{\rm C}$ imaging and photometry

Photometric observations of the young stars in L 1333 in the V, $R_{\rm C}$ and $I_{\rm C}$ bands were undertaken on 2001 October 13, 2003 September 21, and 2004 December 11 using the 1-m RCC-telescope of Konkoly Observatory. In 2001 a Wright Instruments EEV CCD05-20 CCD camera was used, whose pixel size of 22.5 μm corresponded to 0.35 arcsec on the sky. In 2003 and 2004 we used a Princeton Instruments VersArray:1300B camera, that utilizes a back-illuminated, 1300 × 1340 pixels Roper Scientific CCD. The pixel size is 20 μm, corresponding to 0.31 arcsec on the sky. Integration times were between 180 and 600 s. The open cluster NGC 7790 was observed each night several times, at various airmasses, for calibrating the photometry. We reduced the images in IRAF. After bias subtraction and flat-field correction, point spread function (PSF) photometry was performed using the DAOPHOT package. The transformation formulae between the instrumental and standard magnitudes and colour indices as a function of the airmass were established each night by measuring the instrumental magnitudes of some 30 photometric standard stars published by Stetson (2000) for NGC 7790. OKS Hα 6 S was invisible in our V images, thus only its $R_{\rm C}$ and $I_{\rm C}$ could be determined.

The results of the photometry for the three epochs are presented in Table 2. The photometric errors, given in parentheses, are quadratic sums of the formal errors of the instrumental magnitudes and those of the coefficients of the transformation equations. In some cases, magnitudes measured at various epochs differ from each other by more than 0.1 mag. Comparison of the magnitudes of other stars within the field of the target objects has not shown such large discrepancies. Therefore, we conclude that part of these deviations is due to the variability of the stars. In order to determine the interstellar extinction suffered by the stars and their luminosities, we used the averages of the magnitudes presented in Table 2.

Our images have revealed IRAS 02086+7600 to be slightly extended. Small reflection nebulae can be seen next to both OKS Hα 5 and IRAS 02086+7600. We chose PSF photometry in order to minimize the contribution of the extended emission to the resulting magnitudes listed in Table 2.

3 DISCUSSION

3.1 Interstellar extinction and SEDs

We supplemented our observational data with the near-infrared (NIR) data of the 2MASS All Sky Catalog (Cutri et al. 2003) and the far-infrared data of the *IRAS* PSC and FSC in order to characterize the circumstellar environments of our target objects. Other infrared, e.g. *Spitzer* data are not available for these objects. A single object is associated with OKS Hα 6 in both catalogues. The fluxes of the counterparts, 2MASS J 02152532+7635196 and IRAS 02103+7621 are thus combined from the those of both components of the visual double.

We derived the interstellar extinction suffered by our stars based on the assumption that their total emission in the $I_{\rm C}$ band originates from the photosphere (see e.g. Meyer, Calvet & Hillenbrand 1997; Cieza et al. 2005), and the total $E(R_{\rm C} - I_{\rm C})$ colour excess results from interstellar reddening. The unreddened colour indices were adopted from Kenyon & Hartmann (1995) for luminosity classes V and IV, and from Bessell (1979) for OKS Hα 16, whose spectral features indicated a luminosity class III. The extinction A_V was derived from $E(R_{\rm C} - I_{\rm C})$ as $A_V = 4.76 \times E(R_{\rm C} - I_{\rm C})$ (Cohen et al. 1982). For determining the extinction in the other photometric bands, we used the relations $A_{R_{\rm C}} = 0.78\,A_V$, $A_{I_{\rm C}} = 0.59\,A_V$ for the

Table 2. Results of optical photometry.

Star	Band	2001 October 13	2003 September 21	2004 December 11
IRAS 02086	V	–	–	19.65 (0.07)
	R_C	18.28 (0.06)	17.89 (0.04)	17.95 (0.04)
	I_C	16.65 (0.03)	16.36 (0.04)	16.55 (0.04)
OKS Hα 5	V	15.54 (0.05)	–	15.38 (0.04)
	R_C	14.12 (0.04)	14.02 (0.03)	14.03 (0.03)
	I_C	12.57 (0.03)	12.47 (0.03)	12.61 (0.03)
OKS Hα 6 N	V	13.17 (0.03)	13.21 (0.03)	–
	R_C	12.59 (0.03)	12.50 (0.03)	–
	I_C	11.55 (0.02)	11.67 (0.02)	–
OKS Hα 6 S	V	–	–	–
	R_C	–	15.20 (0.10)	–
	I_C	13.86 (0.05)	13.77 (0.05)	–
OKS Hα 16	V	–	17.42 (0.04)	17.55 (0.05)
	R_C	–	15.52 (0.03)	15.48 (0.03)
	I_C	–	13.56 (0.03)	13.55 (0.03)

Table 3. Properties of the pre-main-sequence stars associated with L 1333, derived from spectroscopic and photometric data.

Star	A_V (mag)	$T_{\rm eff}$ (K)	L ($L_\odot$)	Mass ($M_\odot$)	Age (10^6 yr)
IRAS 02086	3.76 (1.2:)	4000	0.86	0.8	1.5
OKS Hα 5	2.57 (0.42)	3570	0.58	0.3	1.0
OKS Hα 6 N	0.71 (0.42)	4060	0.49	0.8	5.0
OKS Hα 6 S	1.29 (0.55)	3410	0.11	0.15	3.0
OKS Hα 16	5.28 (0.50)	3870	0.93	0.4	1.0

optical (Cohen et al. 1982), and $A_J = 0.26\,A_V$, $A_H = 0.15\,A_V$, $A_{K_s} = 0.10\,A_V$ for the NIR. These latter values, slightly different from the standard Rieke & Lebofsky (1985) extinction law, are based on the relations presented for the 2MASS bands by Nielbock & Chini (2005).

This method cannot be applied for IRAS 02086+7600, whose spectral type and thus photospheric colour indices are unknown. We derived the interstellar extinction suffered by this object by assuming that its unreddened position in $J - H$ versus $H - K_s$ colour–colour diagram is on the *T Tauri locus* defined by Meyer et al. (1997), i.e. its colour indices satisfy the relationship $(J - H)_0 = 0.58(H - K)_0 + 0.52$. We also determined A_V by this method for OKS Hα 5 and OKS Hα 16 and found that the results were compatible with those derived from $E(R_C - I_C)$.

The extinctions adopted are listed in column 2 of Table 3. We note that the dereddened colour index $R_C - I_C$ of IRAS 02086+7600 is $(R_C - I_C)_0 = 0.73$, suggesting a ∼ K7-type star, in accordance with the absence of TiO bands in the spectrum.

We constructed the spectral energy distributions (SEDs) of the stars using their magnitudes corrected for the interstellar extinction. The fluxes corresponding to zero magnitude were obtained from Glass (1999) for the VR_CI_C bands, and from the 2MASS All Sky Data release web document[1] for the JHK_s bands. The resulting dereddened SEDs are shown in Fig. 2. In the plots of OKS Hα stars, dashed lines show the SEDs of the photospheres, determined from the dereddened I_C magnitudes and from the colour indices corresponding to the spectral types. The SEDs confirm the CTTS-nature of the OKS Hα stars: their SEDs display significant far-infrared excesses and negative slopes between 2 and 25 μm, characteristic of Class II infrared sources (Lada 1991), i.e. stars surrounded by dusty accretion discs. The plot of OKS Hα 6 shows the sum of both components.

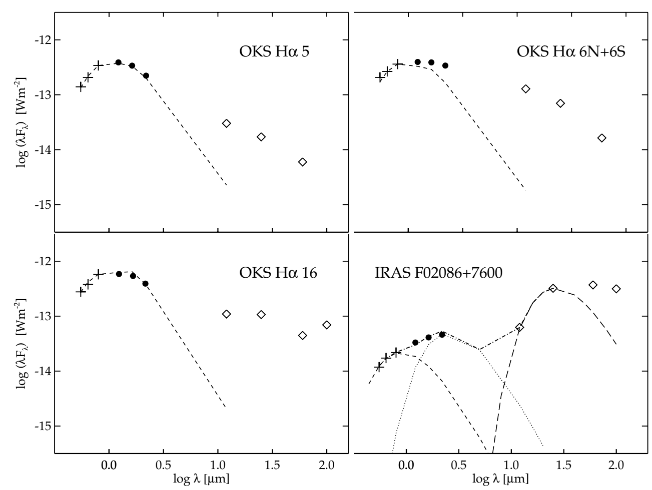

Figure 2. SEDs, corrected for the interstellar extinction, of the YSOs associated with the L 1333 molecular complex. Crosses result from our VR_CI_C photometry, dots come from the 2MASS data and diamonds mark the *IRAS* fluxes. Dashed lines show the contribution of the photoshere to the SEDs of the OKS Hα stars, and a 4000-K blackbody fitted to the optical fluxes of IRAS 02086+7600. In the plot of this latter object, the dotted line shows a 1400-K blackbody and the long-dashed line is a 130-K blackbody. The sum of these three components is drawn by dash–dotted line.

Contrary to the OKS Hα stars, the slope of the SED of IRAS 02086+7600 is $d \log(\lambda F_\lambda)/d \log \lambda = 0.80$ between 2 and 25 μm, characteristic of Class I sources. The shape of the SED over the wavelength interval 0.55–25 μm can be well matched with the sum of three blackbodies, indicated in Fig. 2, and suggesting three

[1] http://www.ipac.caltech.edu/2mass/releases/allsky/doc/sec6_4a.html.

dominant temperatures in the inner regions of the system. The hottest component, fitted to the optical part of the SED (dashed line), has $T \approx 4000$ K and corresponds to the photosphere of a K7-type central star. Ignorance of the contribution of veiling and scattered light to the optical fluxes make this temperature estimate somewhat uncertain. We rely on this value, in view of the observational results that the veiling is constant redward of ~5000 Å (e.g. Basri & Batalha 1990; White & Hillenbrand 2004), and assuming that we were able to exclude a considerable part of the scattered light by performing PSF photometry. The uncertainty, estimated from the goodness of the fit, is ±200 K. The next component of the SED is a blackbody with $T = 1400$ K, quite similar to the spectra of the NIR excesses of CTTSs (Muzerolle et al. 2003), which have been successfully modelled as the 'photosphere' of the inner rim of the disc, emitting like a blackbody near the dust sublimation temperature. The third dominant temperature, suggested by the shape of the SED, is ~130 K. Beyond 25 μm the SED turns flat, suggesting the peak position between 60 and 100 μm.

3.2 Positions of the pre-main-sequence stars in the HRD

Bolometric luminosities of the OKS Hα stars were derived by applying the bolometric corrections BC_{I_C}, tabulated by Hartigan, Strom & Strom (1994) to the dereddened I_C magnitudes, and adopting a distance of 180 pc. The distribution of the stars in the HRD is displayed in Fig. 3. Errors of $\log T_{\rm eff}$ were derived from the accuracy of ±1 spectral subclass of the spectral classification. The error of the luminosity comes from the quadratic sum of $\delta I_C \approx 0.03$, $\delta A_{I_C} \approx 0.42$, $\delta BC_{I_C} \approx 0.01$ and $\delta(5 \log D) \approx 0.08$. The effect of distance uncertainty on the relative positions of the stars was estimated with the assumption that the scatter of the distances of stars is same as their largest projected separation, i.e. ~7 pc.

The luminosity of IRAS 02086+7600 over the wavelength interval 0.55–135 μm was calculated by integrating the available dereddened fluxes. Applying a long-wavelength correction as proposed by Kenyon et al. (1990) for objects with SED peaks near 100 μm, $L_{>135} \approx 0.86\,L_{100}$, and neglecting the luminosity below 0.55 μm,

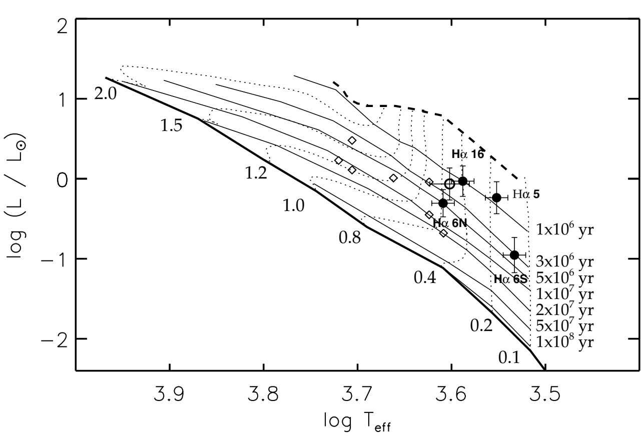

Figure 3. Positions of the young stars of the L 1333 region in the HRD, assuming a distance of 180 pc. Black dots with error bars indicate the CTTSs associated with L 1333, and the open circle shows the estimated position of IRAS 02086+7600. Diamonds indicate the nearby WTTSs identified by Tachihara et al. (2005). Thin solid lines indicate the isochrones as labelled, and dotted lines show the evolutionary tracks for the masses indicated at the lower end of the tracks according to Palla & Stahler (1999) model. The dashed line corresponds to the birthline and thick solid line indicates the zero-age main-sequence.

we obtained a total luminosity of $L_{\rm tot} = 1.04\,{\rm L}_\odot$. In addition to the bolometric luminosity of the central star ($L^*_{\rm bol}$), this total luminosity includes the luminosity of the accretion shock ($L_{\rm acc,shock}$), and those generated and reprocessed in the disc ($L_{\rm acc,disc}$ and $L_{\rm rep,disc}$). In order to obtain $L^*_{\rm bol}$, contributions of $L_{\rm acc,shock}$, $L_{\rm acc,disc}$, and $L_{\rm rep,disc}$ have to be subtracted from $L_{\rm tot}$. To this end we utilized two empirical relationships, resulted from comprehensive studies of large YSO samples. First, it was shown by White & Hillenbrand (2004), that the total luminosity of Class I sources can be approximated as $L_{\rm tot} = 1.08\,L^*_{\rm bol} + 1.58\,L_{\rm acc,shock}$, where $L_{\rm acc,shock} = (GM_*\dot{M})/R_*$. The second relationship is that established by Muzerolle et al. (2003) between $\dot{M}$ and the luminosity of the Ca II λ 8542 line. Following their method, the measured EW(Ca II λ 8542) = 10 Å resulted in $\dot{M} \approx 5.7 \times 10^{-9}$ M$_\odot$ yr^{-1}, comparable to the median value $\dot{M} = 7.9 \times 10^{-9}$ M$_\odot$ yr^{-1}, obtained by White & Hillenbrand (2004) for the Class I objects of Taurus. With the assumptions $M_* = 0.8\,{\rm M}_\odot$, and $R_* = 2\,{\rm R}_\odot$ the obtained mass accretion rate led to $L_{\rm acc,shock} = 0.07\,{\rm L}_\odot$ and $L^*_{\rm bol} = 0.86\,{\rm L}_\odot$. The resulting temperature and luminosity of IRAS 02086+7600 is plotted as the open circle in Fig. 3. The uncertainty was calculated as in the case of OKS Hα stars.

Evolutionary tracks and isochrones, as well as the position of the birthline and zero-age main-sequence (Palla & Stahler 1999) are also shown in Fig. 3. We obtained masses 0.8 and 0.2 M$_\odot$ for OKS Hα 6 N and OKS Hα 6 S, respectively. Our data suggest that within the accuracy both components are coeval, ~3–5 Myr old. OKS Hα 5, OKS Hα 16, and IRAS 02086+7600 lie close to the 10^6-yr isochrone. The weak-line T Tauri stars (WTTSs) identified by Tachihara et al. (2005) near L 1333 are also plotted in Fig. 3 (see Section 3.4). Table 3 summarizes our main results: A_V, $T_{\rm eff}$, $L/{\rm L}_\odot$, as well as the masses in M$_\odot$ and ages in 10^6 yr, read from Fig. 3.

3.3 Large-scale environment of L 1333

The map of the visual extinction of the region $117° \leqslant l \leqslant 135°$ and $+10° \leqslant b \leqslant +17°$, taken from the *Atlas and Catalog of Dark Clouds* by Dobashi et al. (2005) and displayed in Fig. 4, shows that L 1333 is near the middle of a long, diffuse filamentary cloud complex spanning from $l \sim 120°$ to ~134°, far beyond the limits of the molecular observations presented in Paper I. The dark cloud seen at $127° \lesssim l \lesssim 131°$ is catalogued as DUK 853 by Dobashi et al. (2005) and contains eight clumps (*P1–P8* in the order of decreasing mass). L 1333 as catalogued by Lynds (1962) corresponds to the largest clump *P1*. IRAS 02086+7600 and OKS Hα 5 are located at the high-latitude edge of the second largest clump *P2*, and OKS Hα 6 is projected on the edge of the small clump *P7* at the highest latitude side of DUK 853. OKS Hα 16 is projected near the centre of clump *P4* of the same dark cloud. The catalogue of Dobashi et al. (2005) provides an opportunity to derive the masses of the clouds and their clumps. The total mass of the clouds within the diffuse filament between $l \sim 120°$ and ~134°, derived from the visual extinction, is ~2300 M$_\odot$. Clump masses range between 2 and 30 M$_\odot$.

In order to assess the star-forming history of the whole region we also plotted in Fig. 4 the WTTSs identified by Tachihara et al. (2005), and lying far from any dark cloud. Tachihara et al. suggested that the parent clouds of these stars might have been connected to the L 1333 complex. In order to properly compare the ages of these WTTSs with those of our CTTSs, we plotted their data, taken from the table 3 of Tachihara et al. (2005), in Fig. 3 [Tachihara et al. used isochrones of D'Antona & Mazzitelli (1994), giving somewhat different results]. The ages of the WTTSs, assuming a distance of 200 pc, are between

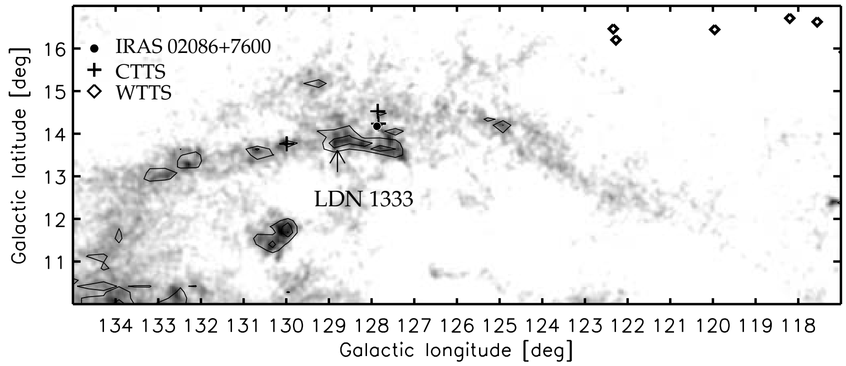

Figure 4. Large-scale distribution of the visual extinction around L 1333, adopted from Dobashi et al. (2005). Contours are drawn at $A_V = 1.0$ and 1.5 mag. YSOs associated with the L 1333 molecular complex, and the WTTSs identified by Tachihara et al. (2005) are indicated.

3 and 10 Myr, with the youngest one at the highest longitude end of the chain, and the oldest on the low-latitude end.

3.4 A possible scenario of star formation

Comparison of the properties of dense $C^{18}O$ cores of L 1333 with those of other nearby star-forming clouds have shown these cores to be smaller and less massive than the similar regions of Taurus, Ophiuchus, Lupus and Chamaeleon clouds (Paper I; Mizuno et al. 1998; Tachihara et al. 2002). Star formation in such an environment is thought to be assisted by some external trigger, and the filamentary clouds themselves have probably been created by large-scale motions of the interstellar gas. The most plausible scenario, suggested by the arc-like structure is, that energetic stellar winds and/or supernova explosions of high-mass stars at lower Galactic latitudes lifted the gas above the galactic plane and compressed it to form stars. In this case the apparent filament is a projection of a shell, and its line-of-sight extent may be comparable to its length. The distribution of YSOs relative to the clouds does not support this scenario. The young stars of L 1333 are located at the high-latitude side of the cloud, with the oldest member, OKS Hα 6, lying farthest from the cloud. The lack of Hα emission stars, as well as YSO-like *IRAS* and 2MASS point sources on the low-latitude side of the filament suggests star formation propagating towards lower latitudes, and a source of trigger at higher Galactic latitudes.

A possible candidate trigger source is the collision of high-velocity gas with the giant radio continuum emitting region *Loop III*, described by Verschuur (1993). Our target objects are located near the far side of Loop III (Berkhuijsen 1971; Spoelstra 1972). Verschuur (1993) has shown that Loop III collided with high-velocity gas originating from a galactic supershell some 7×10^5 yr ago. The collision has been well modelled for latitudes $b > 20^\circ$. At lower latitudes, however, the behaviour of the supershell and its collision with the local interstellar matter have not yet been studied. In order to reveal the geometry of the possible collision in the latitude range 10–20°, the velocity distributions of both molecular and atomic gas have to be studied in detail. Closer to the Galactic plane, the high-velocity gas of the supershell might have decelerated before reaching our Galactic neighbourhood.

In this scenario the high-density regions, created by the colliding surfaces, have small line-of-sight extent. The ages obtained for IRAS 02086+7600, OKS Hα 5 and OKS Hα 16, taking into account their accuracies, support this scenario. OKS Hα 6 was, however, born apparently before the collision. The WTTSs to the west of the cloud complex make the pattern of star formation of this region even more complicated. They indicate a prolonged star formation in the region. The age distribution of the WTTSs suggests star formation propagating from lower to higher Galactic longitudes. More accurate age determinations and more detailed mapping of molecular velocity distribution are needed to clarify the picture.

4 CONCLUSIONS

We identified five low-mass YSOs in the small filamentary molecular complex associated with the dark cloud Lynds 1333. Their masses are in the interval 0.15–0.8 $M_\odot$, and they are 1–5 Myr old. We confirmed that IRAS 02086+7600 is a Class I YSO associated with the L 1333 complex, and found its age to be comparable to those of the CTTSs born in the same cloud. The relative distribution of YSOs and clouds suggests that the star formation might have been triggered by the collision of high-velocity gas with Loop III.

ACKNOWLEDGMENTS

This work is partly based on observations with Nordic Optical Telescope operated on the island of La Palma jointly by Denmark, Finland, Iceland, Norway and Sweden, in the Spanish Observatorio del Roque de los Muchachos of the Instituto de Astrofísica de Canarias. The data presented here have been taken using ALFOSC, which is owned by the Instituto de Astrofísica de Andalucía (IAA) and operated at the Nordic Optical Telescope under agreement between IAA and the NBIfAFG of the Astronomical Observatory of Copenhagen. Our results are partly based on observations obtained at the Centro Astronómico Hispano Alemán (CAHA) at Calar Alto, operated jointly by the Max-Planck Institut für Astronomie and the Instituto de Astrofísica de Andalucía (CSIC). We are indebted to Francesco Palla for sending his data set on pre-main-sequence evolution, and to László Szabados for careful reading of the manuscript. Financial support from the Hungarian OTKA grants T034584, T037508, TS049872, T042509 and T049082 is acknowledged. SN acknowledges support from the Chilean Centro de Astrofísica FONDAP No. 15010003 and Serbian Ministry of Science and Environmental Protection grant No. 146016.

REFERENCES

Basri G., Batalha C., 1990, ApJ, 363, 654
Berkhuijsen E. M., 1971, A&A, 14, 359
Bessell M. S., 1979, PASP, 91, 589

Cieza L. A., Kessler-Silacci J. E., Jaffe D., Harvey P. M., Evans N. J. II., 2005, ApJ, 635, 422
Cohen J. G., Frogel J. A., Persson S. E., Elias J. H., 1982, ApJ, 249, 481
Cutri R. M. et al., 2003, The IRSA 2MASS All-Sky Point Source Catalog, NASA/IPAC Infrared Science Archive. Available online: http://irsa.ipac.caltech.edu/applications/Gator
D'Antona F., Mazzitelli I., 1994, ApJS, 90, 467
de Jager C., Nieuwenhuijzen H., 1987, A&A, 177, 217
Dobashi K., Uehara H., Kandori R., Sakurai T., Kaiden M., Umemoto T., Sato F., 2005, PASJ, 57, S1
Eisner J. A., Hillenbrand L. A., Carpenter J. M., Wolf S., 2005, ApJ, 635, 396
Fujii T., Nakada Y., Parthasarathy M., 2002, A&A, 385, 884
Glass I. S., 1999, Handbook of Infrared Astronomy. Cambridge Univ. Press, Cambridge, p. 63
Hartigan P., Strom K. M., Strom S. E., 1994, ApJ, 427, 961
Hartmann L., 2002, ApJ, 578, 914
Heithausen A., Thaddeus P., 1990, ApJ, 353, 49
Hily-Blant P., Teyssier D., Phillip S., Güsten R., 2005, A&A, 440, 909
Kenyon S. J., Hartmann L., 1995, ApJS, 101, 117
Kenyon S. J., Hartmann L., Strom K. M., Strom S. E., 1990, AJ, 99, 869
Kenyon S. J., Brown D. I., Tout C. A., Berlind P., 1998, AJ, 115, 2491
Kirkpatrick J. D., Henry T. J., McCarthy D. W., 1991, ApJS, 77, 417
Kiss Cs., Moór A., Tóth L. V., 2004, A&A, 418, 131
Koda J., Sawada T., Hasegawa T., Scoville N. Z., 2006, ApJ, 638, 191
Kun M., Prusti T., Nikolić S., Johansson L. E. B., Walton N. A., 2004, A&A, 418, 89
Lada C. J., 1991, in Lada C. J., Kylafis N. D., eds, The Physics of Star Formation and Early Stellar Evolution. Kluwer, Dordrecht, p. 329
Lee C. W., Myers P. C., Tafalla M., 1999, ApJ, 531, 366
Lee C. W., Myers P. C., Tafalla M., 2001, ApJS, 136, 703
Lee C. W., Myers P. C., Plume R., 2004, ApJS, 153, 523
Lynds B. T., 1962, ApJS, 7, 1
Martín E. L., 1997, A&A, 321, 492
Martín E. L., Kun M., 1996, A&AS, 116, 467
Meyer M. R., Calvet N., Hillenbrand L. A., 1997, AJ, 114, 288
Mizuno A. et al., 1998, ApJ, 507, L83
Muzerolle J., Calvet N., Hartmann L., D'Alessio P., 2003, ApJ, 597, L49
Nielbock M., Chini R., 2005, A&A, 434, 585
Obayashi A., Kun M., Sato F., Yonekura Y., Fukui Y., 1998, AJ, 115, 274 (Paper I)
Onishi T., Mizuno A., Kawamura A., Ogawa H., Fukui Y., 1996, ApJ, 465, 851
Palla F., Stahler S. W., 1999, ApJ, 525, 772
Preibisch T., Guenther E., Zinnecker H., 2001, AJ, 121, 1040
Preite-Martinez A., 1988, A&AS, 76, 317
Rieke G. H., Lebofsky M. J., 1985, ApJ, 288, 618
Slysh V. I., Dzura A. M., Valtts I. E., Gerard E., 1994, A&AS, 106, 87
Spoelstra T. A. T., 1972, A&A, 21, 61
Stetson P. B., 2000, PASP, 112, 925
Tachihara K., Onishi T., Mizuno A., Fukui Y., 2002, A&A, 385, 909
Tachihara K., Neuhäuser R., Kun M., Fukui Y., 2005, A&A, 437, 919
Van de Steene G. C., Pottasch S. R., 1995, A&A, 299, 238
Verschuur G. L., 1993, ApJ, 409, 205
White R. J., Basri G., 2003, ApJ, 582, 1109
White R. J., Hillenbrand L. A., 2004, ApJ, 616, 998